Modelling of grain crushing and debonding

Modélisation de l'écrasement des grains et de leur perte d'adhérence

J.Boháč – *Charles University, Dept. of Engineering Geology, Prague, Czech Republic*
J.Feda – *Academy of Sciences, Inst. of Theoretical and Applied Mechanics, Prague, Czech Republic*
B.Kuthan—*Charles University, Dept. of Engineering Geology, Prague, Czech Republic*

ABSTRACT: Silicagel was used to model particle breakage in the laboratory since it exhibited intense grain crushing at pressures lower by an order of magnitude in comparison with silica sand. In the oedometer, particle breakage of spherical particles was observed at vertical effective stresses of about 4 MPa. The collapsible behaviour of the oedometer specimens was modelled numerically by PFC^{2D}. The process of debonding was physically modelled by testing lean mixture of sand and Portland cement in the shear box. Debonding surface which was identified for different cement contents, porosities and gradings makes the Mohr-Coulomb strength envelope a composite one.

RÉSUMÉ: Un gel de silice a été utilisé en laboratoire pour étudier la rupture des particules. Dans un oedomètre, la rupture de particules sphériques a été observée à des contraintes verticales de l'ordre de 4 MPa. Le comportement des échantillons dans l'oedomètre a été modélisé de manière numérique par PFC^{2D}. Le processus de perte d'adhérence cimentation a été modélisé physiquement en testant un mélange maigre de sable et de ciment Portland à l'oedomètre. Le concept de surface d'adhérence, qui fait de l'enveloppe de rupture de Mohr-Coulomb une surface composée (ligne droite + courbe) est proposé.

1 INTRODUCTION

Both particle breakage and cementation are structural effects that have a feature in common: they are associated with substantial adaptation of the soil structure. The process can have a form of a gradual structural change, manifested for example as a mere yield point on the stress-strain curve of a cemented specimen during debonding. Alternatively, the structural modification can be more dramatic, which is the case of subsidence caused by crushing of grains. This kind of behaviour is dealt with in the paper.

2 GRAIN CRUSHING

Crushing of grains is an important phenomenon of the mechanical behaviour of soils. It is often associated with calcareous organic sediments, or granite eluvium. Disintegration of structural units similar to grain crushing may also be expected in the case of anthropogenic deposits, for example non-engineered fills of clayey overburden of coal mines. Particle breakage however seems a general feature of the behaviour of soils. It has been shown recently, that particle breakage is common to all sands (Coop, 1999).

Grain crushing is promoted by grains' angularity, coarseness, uniformity of gradation, low strength (for example with double porosity materials), by the stress level and anisotropy. The most important factor however is the resistance of grains: crushing of quartz sand starts at the stress of 10 to 15 MPa, while calcareous shells start crushing at 50 to 200 kPa, depending on the grain size and porosity (Beringen et al., 1981; Valent et al., 1981). On crushing, fines are produced and grain size distribution curve becomes less steep. Consequently the soil becomes resistant to crushing. Grain size distribution is a suitable measure of the extent of crushing (Hardin, 1985).

Since particle breakage represents a substantial intervention into the soil structure, it results in a modification of the mechanical response of the soil. Firstly, due to the selective grain crushing Mohr-Coulomb peak strength envelope becomes curved, and the peak angle of friction may drop substantially (e.g., Valent et al, 1981). Some researchers found also the critical state line curved due to the grain crushing, others however argue that the apparent nonlinearity is a result of incomplete testing, and that φ'_{cr} is a true constant (Coop, 1999). From the point of view of compressibility, crushing is one of the factors leading to different kinds of structural collapse, including subsidence.

In the laboratory, crushing of granular soils was modelled by oedometer testing of granulated silicagel ($SiO_2.nH_2O$). Numerically was the behaviour modelled by distinct element method using PFC^{2D}.

2.1 Laboratory tests

The grain size of the tested silicagel was 2 to 4 mm. Both angular and spherical grains were tested. Figures 1 and 2 show silicagel spherical particles before and after a test in which a substantial particle breakage and structural collapse took place. The specimens were tested after oven drying at 105°C, and the maximum temperature difference during the tests was 1°C. The maximum difference between the initial and final water contents was 0.5%. The initial porosity of the specimens was 42 to 44%. The tests were carried out in a conventional incremental loading oedometer, allowing the maximum vertical pressure of 6.5 MPa.

During the incremental loading, at the effective vertical stress of about 3.7 to 4.8 MPa all specimens underwent significant structural collapse due to particle breakage (Figure 3). After the

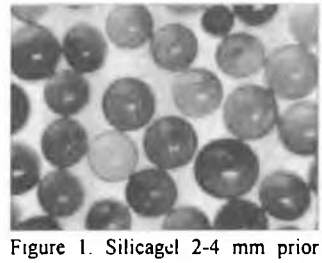

Figure 1. Silicagel 2-4 mm prior oedometer testing.

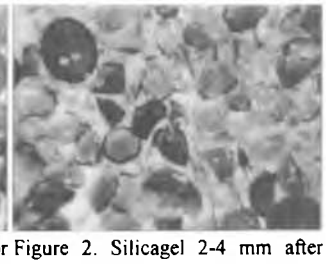

Figure 2. Silicagel 2-4 mm after oedometer testing.

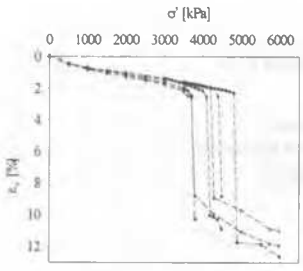

Figure 3. Laboratory compression curves.

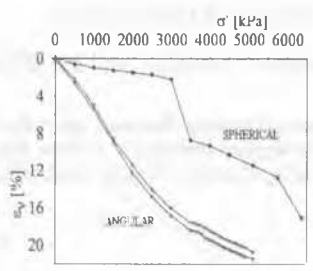

Figure 4. Compression of angular and spherical grains.

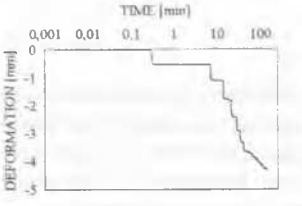

Figure 5. Laboratory settlement vs. time curve for angular grains.

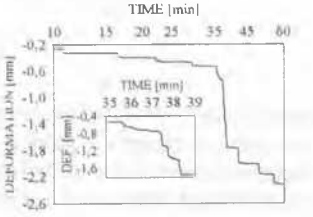

Figure 6. Laboratory settlement vs. time curve for spherical grains.

structural collapse took place, tests were either terminated to determine the grain size distribution, or continued (Figure 3) up to the load of about 5 to 6 MPa.

Only one specimen however was loaded far enough to experience a further major collapse by particle breakage. This can be seen in Figure 4 together with compression curves of two specimens of angular silicagel. Although the extent of grain crushing was higher, as expected, no substantial collapse was observed for angular silicagel. Despite the higher particle breakage, and higher compressibility, the compression curve of angular grains is more or less smooth. The figure indicates that the mechanisms of modification of the soil structure and of particle breakage are different for angular and spherical particles.

The phenomenon is also presented by Figures 5 and 6 showing the dependence of displacement on time for the angular and spherical grains, respectively. At every load increment, the angular grains undergo particle crushing, no subsidence occurs, though, the soil structure is modified at each loading step. However the mechanism of crushing of spheres is different and leads to a sudden subsidence. The detail in Figure 6 shows the development of the subsidence collapse of spherical grains at the constant vertical load.

Three segments can be distinguished on compression lines of collapsible spherical grains: in the first one the avarage compression index $C_c = 0.03$, in the final part after the collapse $C_c = 0.23$. During subsidence due to collapse, by definition $C_c \rightarrow \infty$. For angular grains of Figure 4, $C_c = 0.3$ in the whole testing range.

The extent of particle breakage was quantified by index of crushing I_c, which is defined as the ratio of the area below the grain size distribution curve prior and after the test. For tests in Figure 4, the index of crushing of angular silicagel was 2.07 while for spherical grains $I_c = 2.03$.

2.2 Numerical modelling

The particle breakage observed in the laboratory was modelled numerically by distinct element method, using PFC^{2D}. In total about 50 numerical tests were carried out, looking at the influence of the type of bonding (contact bonds vs parallel bonds; Itasca, 1999), coefficient of friction, damping, normal and shear strength of the bonds, their stiffnesses, etc.

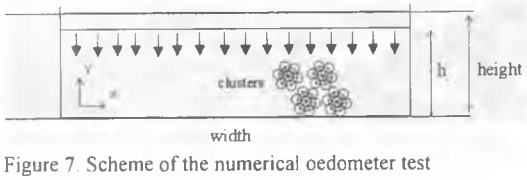

Figure 7. Scheme of the numerical oedometer test

The numerical oedometer tests were set up according to Figure 7. The geometry of the two-dimensional model corresponds with the cross section of the oedometer apparatus. The grains of silicagel were modelled by two-dimensional clusters of 7 individual disks - basic particles available in PFC^{2D}. The numerical tests were realized by means of a servomerchanism with predefined target vertical stress of 6 MPa. The average initial and final porosities, which however can hardly be related to the porosity of the three-dimensional physical models, were 34% and 22%, respectively.

Similarly to the physical oedometer tests (Figure 3), three basic segments of compression curves were distinguished. The values of compressibility parameters as well as the extent of particle breakage depend obviously on the parameters of the model.

The influence of both normal (tensile) and shear strength of the bonds was numerically tested by starting with their initial values of 1×10^8N and by decreasing one of the quantities gradually to 1/700 of its initial value while the other was kept constant. This parametric study was carried out for both contact and parallel bonds. A similar approach was adopted in the case of stiffnesses of the particles, coefficient of friction and damping.

The influence of normal (tensile) strength for both contact and parallel bonds on grain size distribution can be seen in Figure 8. It is based on granulometric classes defined by the numbers of basic particles that remain in the clusters. Strong breakage was observed for numerical specimens with contact bonds of normal strength 5×10^5N and shear strength 1×10^6N, particle friction coefficient 1.0 and damping factor 0.7.

In Figure 9 there is a dramatic breakage of bonds (collapse), numerically modelled at the vertical load of about 3.7 MPa. The result has however been achieved by the contact bonds model with normal strength of 2.5×10^5, at which the compressibility is too high in comparison with physical tests.

Figure 10 shows the best fit achieved by numerical test from the point of view of oedometer modulus and of subsidence due to particle breakage. Full circles depict the physical test on spherical silicagel. Heavy full line represents a contact bonds numerical model with stiffness 1×10^{10} Nm^{-1}. By contact bonds and friction 1.0, a collapse at the stress level similar to that observed in the physical test was achieved; the numerical compressibility is however higher. Dotted line is for parallel bonds with particle stiffnesses 5×10^9 Nm^{-1}: the compressibilities before and after collapse are realistic, the colapse, though, occurred at lower stress than in the laboratory.

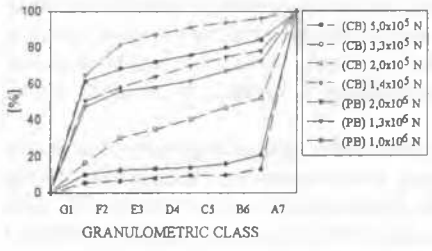

Figure 8. Numerical grading curves.

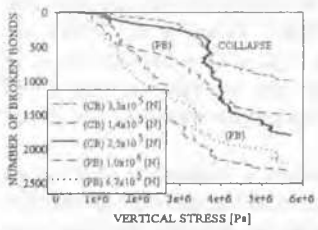

Figure 9. Numerical compression curves.

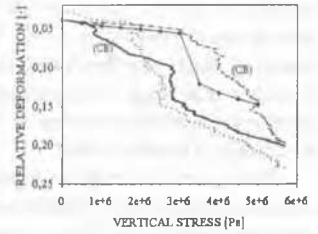

Figure 10. Comparison of numerical compression curves with experiment.

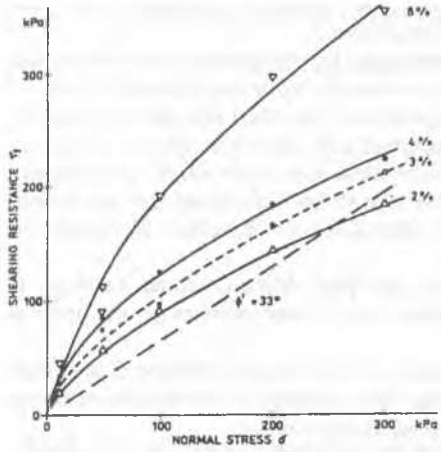

Figure 11. Non-linear shear strength envelopes for sand cemented by 2% to 8% of Portland cement (Feda, 1998).

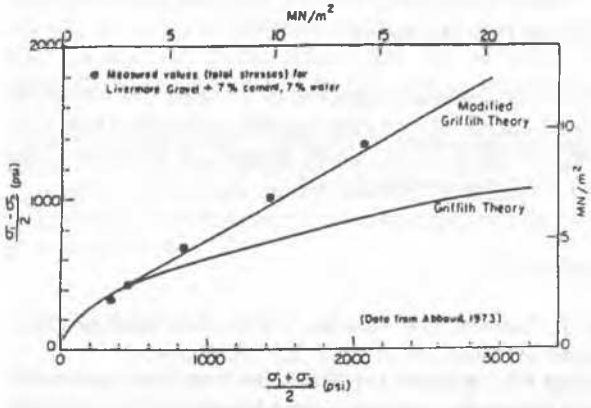

Figure 12. Strength envelopes of cement-treated gravel: experiments and Griffith theory (Mitchell, 1976).

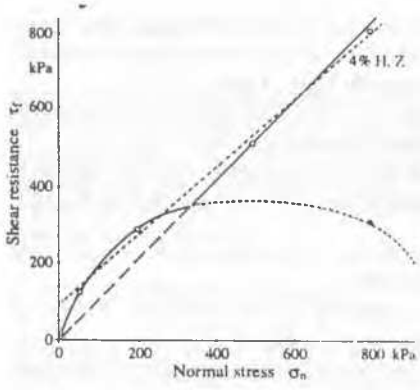

Figure 13 Shear strength and two interpretations of the strength envelope of dense saturated sand with 4% of cement.

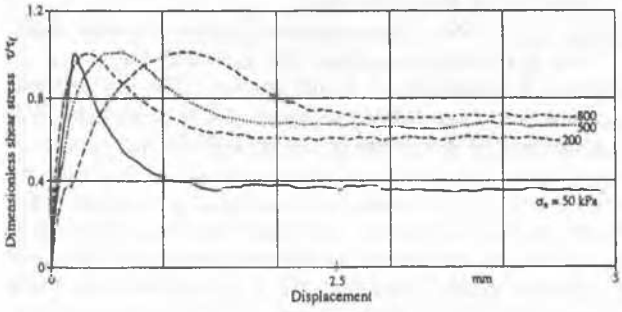

Figure 14. Dimensionless stress-strain diagrams of tests from Figure 13.

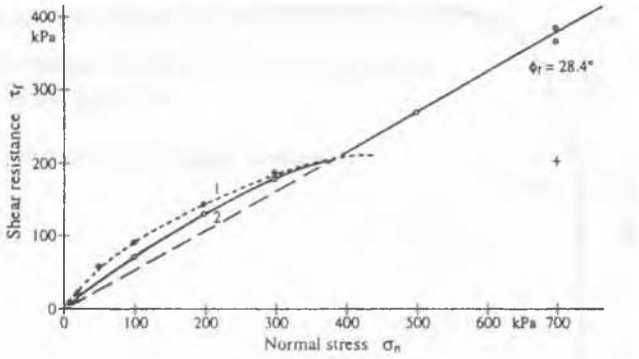

Figure 15. Effect of initial porosity on debonding surface of sand treated by 2% of cement. 1: $n_0 \doteq 50\%$, 2: $n_0 \doteq 55\%$.

3. DEBONDING

Solid structural units of soils seldom interact solely by contact forces. Usually they are cemented by various types of natural cement, for example carbonates, silicates, clay minerals, iron or magnesium oxides etc. Bonds are recognized to represent the principal structure-forming factors of natural soils (see, e.g., Leroueil & Vaughan, 1990). In addition to natural bonding soils can be artificially cemented due to the improvement technique of stabilizing by Portland cement or lime.

However, cementation increases soil's potential to collapse: if there is a failure of the bonds, metastable soil structure results leading to structural collapse. Therefore studying cementation and debonding is important for understanding collapsibility of soils.

To investigate the mechanism of bonding due to cementation and its effect on the soil strength, mixtures of sand and Portland cement were tested. Reconstituted specimens were prepared from two kinds of alluvial quartz sand, with grains 0.1 to 2 mm and 0.1 to 4 mm, both of minimum and maximum porosity of about 35% and 46%. Dry sand was mixed with 2%, 3%, 4% and 8% by weight of cement, 8% of distilled water added (by weight of dry sand). After curing for 5 days at constant water content specimens were oven-dried at 60°C and sheared at constant rate of shear displacement of 0.05 mm per minute in the shear box.

Generally, by cement admixture deformation properties of soils are improved. For example, on increasing cement content from 1% to 5% by weight, small strain modulus may increase by about one order of magnitude (Baig et al., 1997). Admixture of cement is often evaluated as an increase of cohesion, the effect on friction angle being considered small. However the peak strength of cemented soil is represented better by a curved Mohr-Coulomb strength envelope (Figure 11), alternatively by using a modified Griffith crack theory to explain the transition from the nonlinear envelope for low stress level to the linear one at the higher stress (Figure 12).

Empty circles in Figure 13 show peak failure of four shear box tests on dense sand with 4% of cement, tested water saturated. There are two alternatives of interpreting the results. The first one is a conventional Mohr-Coulomb envelope, i.e., a linear strength envelope shown by the dotted straight line, $\varphi_p' = 41.5°$, $c_p' = 9$ kPa. The second one is a composite envelope consisting of a nonlinear segment at the lower stress range, i.e. for normal stress up to about 350 kPa, and of a straight line at higher stresses, which is shown by a full line in the figure ($\varphi_p' \doteq 45°$).

In Figure 14 there are dimensionless stress-strain diagrams of the tests shown in Figure 13. Since the dimensionless stress-strain diagrams do not coincide, the behaviour of the specimens is not physically identical and the linear strength envelope in Figure 13 is incorrect. Instead, the nonlinear envelope, which is a part of

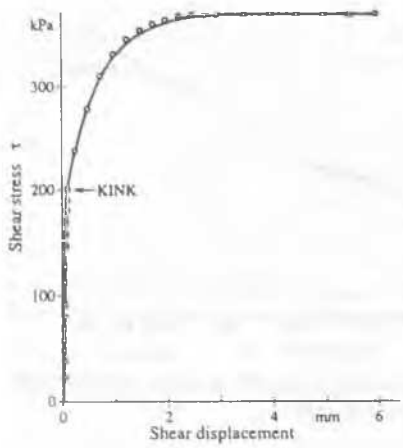

Figure 16. Identifying the point of debonding <+> of Figure 15.

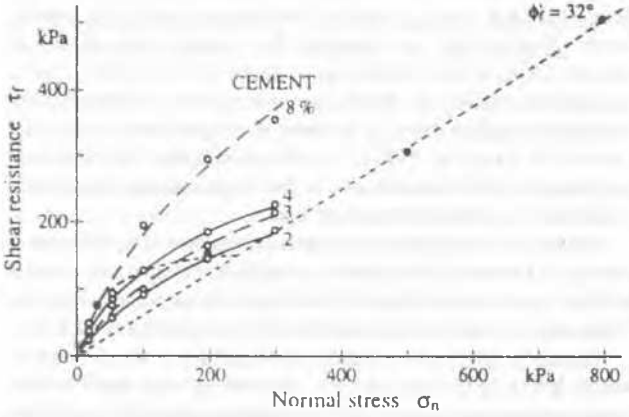

Figure 17. Effect of the amount of cement on debonding surface.

debonding surface is preferable for interpreting shear strength of cemented soils.

The points of the debonding surface can be identified as yield points (Coop & Atkinson, 1993). An example is in Figures 15 and 16. There are debonding curves for two series of sand specimens of different porosities in Figure 15: 1 represents debonding surface for porosity approximately 50% and 2 debonding surface for porosity 55%. Debonding point shown by the cross in Figure 15 corresponds to the yield point (kink) on the stress-strain diagram in Figure 16.

The influence of the amount of cement on the debonding surface can be seen in Figure 17, where empty circles show results of tests with 2%, 3%, 4% and 8% of cement admixture. Full circles represent the second type of sand, with grains up to 4 mm, with 2% of cement. The difference between the debonding surface of the two sands at the same mixing ratio indicates the possible effect of grain size distribution.

CONCLUSIONS

In laboratory incremental oedometer tests, grains of angular model material - silicagel - exhibited particle breakage during the whole loading process. The modification of the structure took place gradually without a dramatic subsidence due to particle breakage.

Specimens of spherical silicagel experienced a clear subsidence due to grain crushing at the vertical load of about 4 MPa.

The tests indicated, that despite the apparently higher compressibility and higher (gradual) grain crushing of the angular grains, the compression lines of both angular and spherical material were likely to converge at a stress closely above the maximum experimental pressure. Although the mechanism of particle breakage is different, the index of crushing and total compressibility are comparable.

By PFC^{2D}, collapses due to particle breakage were successfully modelled. The work continues by modelling angular particles.

For realistic interpretation of the shear strength, the nature of stress-strain diagrams needs to be taken into account. If they are identical in the dimensionless form (normalized, or physically isomorphous behaviour) the Mohr-Coulomb strength envelope is linear. Peak linear Mohr-Coulomb envelope is typical for debonded materials.

For bonded soils, the peak Mohr-Coulomb envelope is composite, i.e. nonlinear in the lower stress range and linear at higher stress.

The nonlinear segment of the strength envelope is associated with gradual debonding of the cemented soil. Within this particular stress interval the soil behaviour is brittle.

Contrary to common yield surfaces, debonding surface is immobile and irreversible.

ACKNOWLEDGEMENT

The work was financially supported by the Grant 103/00/1043 of the Grant Agency of the Czech Republic and by the Grant CEZ J13/98:113100005 of the Czech Ministry of Education. This support is gratefully acknowledged.

REFERENCES

Baig, S., Picornell, N. & Nazarian, S. 1997. Low strain moduli of cemented sands. *JGGE ASCE* 123 (6): 540-545.

Beringen, F. L., Kold, H. J. & Windle, D. 1981. Cone penetration and laboratory testing in marine calcareous sediments. *ASTM Spec. Publ. 777.* Demars, K. R. & Chaney, R. C. (eds.), 179-209.

Coop, M. R. 1999. The influence of particle breakage and state on the behaviour of sands. *Proc. 2nd Int. Workshop on Crushable Soils*, July '99, Yamaguchi Univ., Japan, in press.

Coop, M.R. & Atkinson, J.H. 1993. The mechanics of cemented carbonate sands. *Géotechnique* 43(1): 53-67.

Feda, J. 1998. Bonding of a cement treated sand. *Acta Technica CSAV*, Inst. of Electrical Eng. Acad. Sci. Czech Rep. 43, 189-203.

Feda, J. 2000. A study of soil cementation. *Engineering mechanics*, 7(4): 283-290.

Hardin, B. O. 1985. Crushing of soil particles. *Journal of Geotechnical Engineering* 111(10): 1177-1192.

Itasca, 1999. Particle flow code in 2 dimensions. Itasca Consulting Group Inc., Minesota, USA.

Leroueil, S. & Vaughan, P. R. 1990. The general and congruent effects of structure in natural soils and weak rocks. *Géotechnique* 40(3): 467-488.

Mitchell, J. K. 1976. The properties of cement stabilized soils. *Proc. Res. Work. Leura*, Aus. Sept. 6-10, 365-404.

Valent, P. J., Altschaeffl, A. G. & Lee, H. J. 1981. Geotechnical properties of two calcareous oozes. *ASTM Spec. Publ. 777.* Demars, K. R. & Chaney, R. C. (eds.), 79-96.